Cell Death and Differentiation (1998) 5, 321 – 329

http://www.stockton-press.co.uk/cdd

Relation of impaired energy metabolism to apoptosis and necrosis following transient cerebral hypoxia-ischaemia

Huseyin Mehmet[1], Xue Yue[1], Juliet Penrice[2], Ernest Cady[3], John S. Wyatt[2], Catherine Sarraf[4], Marion Squier[5] and Anthony D. Edwards[1,6]

[1] Department of Paediatrics and Neonatal Medicine, Royal Postgraduate Medical School, London
[2] Department of Paediatrics, University College London
[3] Department of Medical Physics and Bioengineering, University College London, London
[4] Department of Histopathology, Royal Postgraduate Medical School, London
[5] Department of Neuropathology, Radcliffe Infirmary, Oxford
[6] corresponding author: Professor A.D. Edwards, Weston Laboratory, Department of Paediatrics and Neonatal Medicine, Royal Postgraduate Medical School, Du Cane Rd, London W12 ONN. tel: 0181 383 3326; fax: 0181 740 8281; email: dedwards@rpms.ac.uk

Received 2.7.97; revised 7.11.97; accepted 19.11.97
Edited by R.A. Knight

Abstract

This study investigated whether both mild and severe hypoxia-ischaemia (HI) caused significant numbers of cells to die by apoptosis in the developing brain *in vivo*. Newborn piglets were subjected to transient global HI and the fraction of all cells in the cingulate gyrus that were apoptotic or necrotic counted 48 h after resuscitation. The mean (S.D.) proportion of apoptotic cells was 11.9% (6.7%) (sham operated controls 4.1% (2.7%)), while 11.4% (8.4%) were necrotic (controls 0.7% (1.3%)) ($P < 0.05$). Apoptotic and necrotic cell counts were both linearly related to the severity of impaired cerebral energy metabolism measured by magnetic resonance spectroscopy ($P < 0.05$), as shown by: (1) the decline in the ratio of nucleotide triphosphates to the exchangeable phosphate pool during HI; (2) the fall in the ratio of phosphocreatine to inorganic phosphate 8 – 48 h after HI; and (3) an increased ratio of lactate to total creatine at both these times. Thus both apoptosis and necrosis occurred in the cingulate gyrus after both severe and mild HI *in vivo* in proportion to the severity of the insult.

Keywords: brain; newborn; apoptosis; MRS; cerebral energy metabolism

Abbreviations: HI, Hypoxia-ischaemia; MRS, Magnetic resonance spectroscopy; Lac, Lactate; Cr, Total creatine-containing compounds; PCr, Phosphocreatine; Pi, Inorganic phosphate; EPP, Exchangeable phosphate pool; NTP, Nucleotide triphosphates; pH_i, Intracellular pH; ISEL, *in situ* end-labelling of fragmented DNA

Introduction

The changes in cerebral energy metabolism associated with hypoxia-ischaemia (HI) to the developing brain are complex. During HI there is a decline in the cerebral concentration of high energy phosphates and an increase in cerebral lactate (Lac) concentration that recovers soon after resuscitation. However, despite restored substrate delivery, some 8 – 12 h later a delayed phase of reduced phosphorylation potential and increased Lac concentration begins (Vannucci *et al*, 1994; Lorek *et al*, 1994; Penrice *et al*, 1997; Azzopardi *et al*, 1989; Martin *et al*, 1996; Hanrahan *et al*, 1996). The degree of delayed impairment of cerebral energy metabolism predicts the severity of later neurodevelopmental impairment in newborn human infants (Roth *et al*, 1992), and also the severity of histological injury in newborn piglets (Mehmet *et al*, 1994; Yue *et al*, 1996) and rat pups (Blumberg *et al*, 1996).

Apoptosis has been detected in the brains of several mammalian species, including human infants, after HI (Linnik *et al*, 1993; MacManus *et al*, 1993, 1995; Mehmet *et al*, 1994; Li *et al*, 1995; Beilharz *et al*, 1995; Chariaut-Marlangue *et al*, 1995; Edwards *et al*, 1997; Yue *et al*, 1996). Recent *in vitro* data have stressed the role of energy metabolism and the mitochondria in controlling apoptosis (Liu *et al*, 1996; Yang *et al*, 1997), but suggested that apoptosis results from a mild cellular insult, while severe stress induces necrosis (Ankarcrona *et al*, 1995; Bonfoco *et al*, 1995). If these results also applied to intact brain *in vivo*, they would have important implications for the development of neural rescue therapies. However a preliminary quantitative study of the brains of newborn piglets *in vivo* found that the more severe the HI, the greater the increase in apoptosis (Mehmet *et al*, 1994).

This led us to investigate quantitatively the relations between apoptosis, necrosis and the severity of HI to the intact developing brain *in vivo*. The aim of the study was to determine whether both mild and severe HI caused significant numbers of cells in the developing brain to die by apoptosis.

The study used a porcine model of neonatal hypoxic-ischaemic cerebral injury in which cerebral energy metabolism was observed by ^{31}P and ^{1}H magnetic resonance spectroscopy (MRS) both during HI and during the delayed period of energy depletion. Measurements were made of 4 MRS variables:

(1) The ratio of phosphocreatine to inorganic phosphate ([PCr]/[Pi]) was measured by ^{31}P MRS as the most sensitive indicator of cerebral phosphorylation potential during the delayed phase of injury.
(2) ^{31}P MRS was also used to measure relative concentrations of nucleotide triphosphates (NTP), which consist mainly of ATP, expressed as a fraction of the total exchangeable phosphate pool [EPP], which was defined as the sum of the phosphorylated metabolites most directly involved in energy metabolism and derived from the equation $[EPP]=[Pi]+[PCr]+[(\alpha+\beta+\gamma)\text{-}NTP]$. This provided the best available index of falling [ATP]. The time integral of the decline in [NTP]/[EPP] was used as a measure of the severity of the acute insult during HI and in the first hour after resuscitation.
(3) In four sham-operated control piglets and five of the HI

group glycolytic metabolism was observed by ^{1}H MRS measurements of the peak-area ratio of Lac to total creatine (Cr), which comprised of Cr and PCr (Cady, 1994).

(4) Intracellular pH (pH_i) was measured to confirm the expected difference between acute HI when pH_i is low, and delayed dephosphorylation when it is almost normal or increased. The Henderson-Hasselbach relationship was applied to determine pH_i from the chemical shift of Pi relative to PCr (Petroff *et al*, 1985).

Apoptosis and necrosis were quantitated 48 h following HI by classifying and counting dead cells on the basis of morphology. The quantitative relations between modes of cell death and impaired cerebral energy metabolism were then examined.

Results

MRS measurements of hypoxia-ischaemia

Carotid artery occlusion and hypoxia was continued for mean 60.6 (S.D. 11.0) min. MRS data obtained from experimental subjects and controls are given in the Table. During HI [PCr]/[Pi], [NTP]/[EPP] and pH_i became significantly lower, and Lac/Cr significantly higher, than baseline or in control subjects. As in previous reports (Lorek *et al*, 1994), these variables all returned close to baseline and control values upon resuscitation (data not shown). During the following 48 h [PCr]/[Pi] and [NTP]/[EPP] declined to levels significantly lower than baseline or control values, and Lac/Cr became significantly greater than baseline or controls. As expected, these MRS variables were significantly correlated to each other. pH_i did not decline during the secondary phase of injury, remaining similar to baseline and control values.

Cellular morphology

Forty-eight hours after transient HI light microscopy demonstrated both apoptotic and necrotic cells in the crest and sulcus of the cingulate gyrus. The distribution of dead cells was non-uniform, and apoptotic and necrotic cells were characteristically seen next to each other in the same field (Figure 1A).

Electron microscopy showed that apoptotic cells typically contained electron dense nuclei (Figure 1B). Occasionally chromatin 'caps' could be detected, with the nuclear envelope becoming somewhat dilated. The cytoplasmic volume of apoptotic cells was generally reduced and organelles, although intact, were tightly packed together in a distinctive fashion. In contrast, necrotic cells often displayed a significant increase in cytoplasmic volume accompanied by a loss in the integrity of all cellular membranes. The nuclear envelope of a necrotic cell was typically ruptured, resulting in the leakage of chromatin into the cytoplasm, where swelling of mitochondria and endoplasmic reticulum and the appearance of numerous large vacuoles were also clearly visible (Figure 1C).

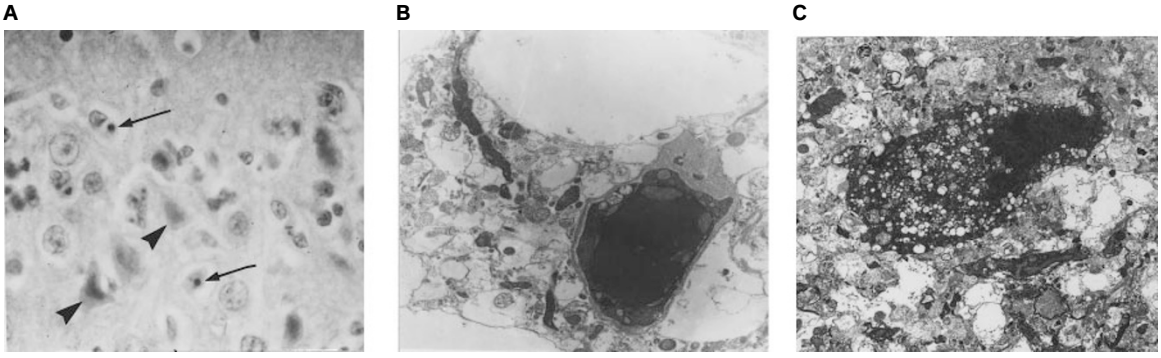

Figure 1 Histological appearance of cells in the cingulate gyrus of a newborn piglet 48 h following hypoxic-ischaemic injury. (**A**) Paraffin sections (5 μM) stained with haematoxylin and eosin, containing cells with the typical morphological characteristics of apoptosis (arrow) or necrosis (arrowhead). Magnification: $\times$230. (**B**) Electron micrograph of a cortical neuron undergoing apoptosis, showing characteristic cytoplasmic shrinkage and condensation of chromatin within the nucleus. Magnification: $\times$5280. (**C**) Electron micrograph of a cortical neurone undergoing necrosis, showing an enlarged nucleus containing dispersed chromatin and the widespread disruption of organelles within the cytoplasm. Magnification: $\times$2650

Table 1

	pH_i (before HI)	pH_i (during HI)	pH_i (48 h after HI)	$_0]^t\Delta$[NTP]/[EPP]dt	[PCr]/[Pi]min (after HI)	[Lac]/[Cr] max (before HI)	[Lac]/[Cr] max (during HI)	[Lac]/[Cr] max (48 h after HI)
HI	7.05 (0.03)	6.176 (0.57)	7.07 (0.07)	0.091 (0.04)	0.62 (0.51)	0.22 (0.18)	1.96 (0.95)	1.733 (0.94)
Control	7.032 (0.22)	–	7.06 (0.02)	0	1.14 (0.45)	0.27 (0.21)	–	0.142 (0.09)
HI v Controls	NS	p<0.05*	NS	p<0.05	p<0.05	NS	p<0.05*	p<0.05

Indices of cerebral energy metabolism before, during and after hypoxia-ischaemia measured by magnetic resonance spectroscopy, given as mean (standard deviation). HI=hypoxia-ischaemia; pH_i=intracellular pH; $_0]^t\Delta$[NTP]/[EPP]dt=time integral of the fall in the ratio of nucleotide triphosphate to exchangeable phosphate pool; [PCr]/[Pi]min=minimum ratio of phosphocreatine to inorganic phosphate recorded during delayed phase of impaired energy metabolism; Lac/Cr max=maximum value of the ratio lactate to total creatine. *=significant difference between HI value, and both control and HI group baseline values (P<0.05)

Quantitation of cell death

In animals subjected to HI the mean proportion of apoptotic cells was 11.9% (S.D. 6.7%), and a similar proportion, 11.4% (8.4%), was necrotic. Significantly fewer dead cells were seen in sham operated controls, where 4.1% (2.7%) of cells were apoptotic, and 0.7% (1.3%) necrotic ($P<0.05$). A small number of cells, always fewer than 10% of the total cell count, were of indeterminate morphology and these were excluded from counting.

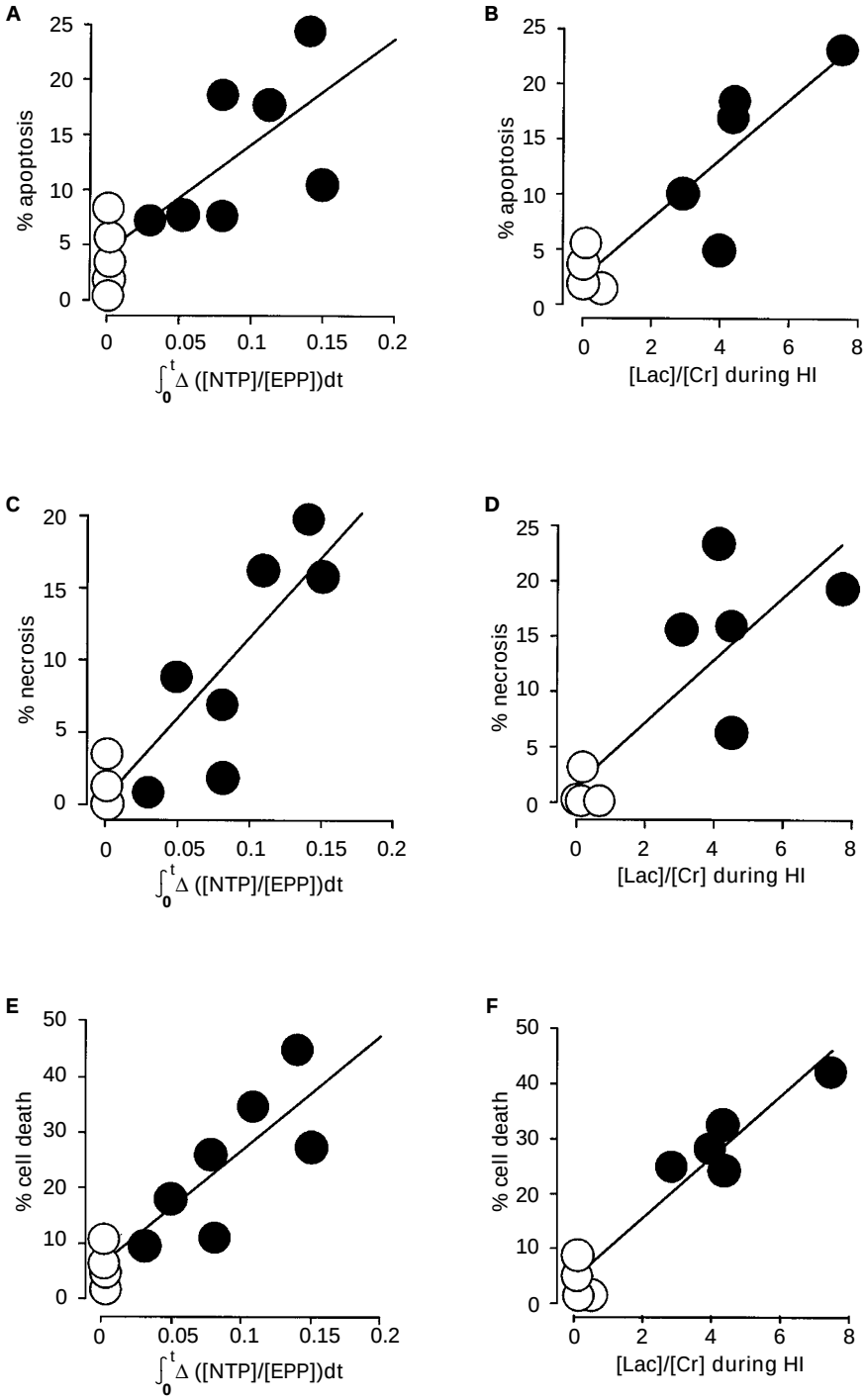

Figure 2 Relations between the proportions of cell death in the cingulate gyrus and energy depletion during hypoxia-ischaemia (HI). Column 1: the relation between the time integral of the fall in the ratio of nucleotide triphosphate: exchangeable phosphate pool ($_0\int^t\Delta$[NTP]/[EPP]dt) and apoptosis (**A**), necrosis (**C**), and total cell death (**E**). Column 2: the relation between the ratio of lactate to creatine ([Lac]/[Cr]) and apoptosis (**B**), necrosis (**D**), and total cell death (**F**). Symbols: open circles, sham-operated controls; filled circles, hypoxic-ischaemic group. Some data points are superimposed. Least-square linear regression lines are shown ($P<0.025$)

Relations of cell death and impaired cerebral energy metabolism

The proportions of apoptosis, necrosis and total cell death were all significantly related to the severity of HI, measured as the time integral of the fall in [NTP]/[EPP] (Figure 2A, C, E) and the maximum value of Lac/Cr observed during HI (Figure 2B, D, F) ($P < 0.05$).

Total cell death, apoptosis and necrosis were also significantly related to the severity of delayed energy

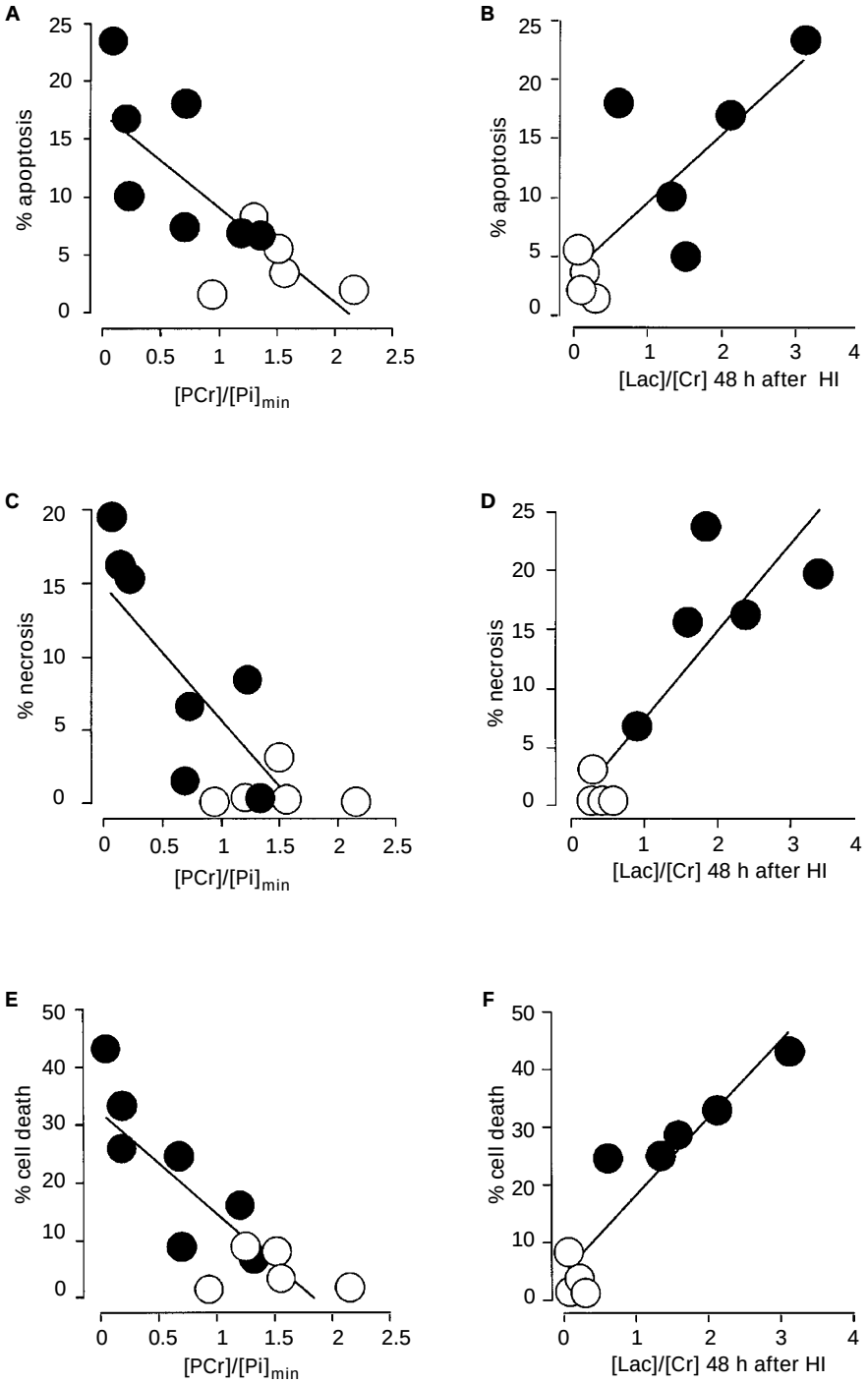

Figure 3 Relations between the proportions of cell death in the cingulate gyrus and energy depletion during the delayed phase of injury. Column 1: the relation between the concentration ratio of phosphocreatine to inorganic phosphate ([PCr]/[Pi]) and apoptosis (**A**), necrosis (**C**), and total cell death (**E**). Column 2: the relation between the ratio of lactate to creatine ([Lac]/[Cr]) and apoptosis (**B**), necrosis (**D**), and total cell death (**F**). Symbols: open circles, sham-operated controls; filled circles, hypoxic-ischaemic group. Some data points are superimposed. Least-square linear regression lines are shown ($P < 0.025$)

failure, measured by the nadir of the ratio [PCr]/[Pi] (Figure 3A, C, E) and the ratio Lac/Cr 48 h after the resuscitation (Figure 3B, D, F ($P<0.025$).

There was also a significant inverse linear relation between the proportion of all cell death that was due to apoptosis, and the severity of HI ($P<0.025$). In subjects with very mild insults apoptosis accounted for almost all cell death, while the proportion fell progressively with more severe HI so that in subjects enduring the most severe dephosphorylation necrosis accounted for approximately half of all cell death (Figure 4).

In six of the subjects the number of apoptotic cells was also estimated by counting the number of cells that demonstrated *in situ* end labelling of fragmented DNA (ISEL). Although the proportion of ISEL positive cells was always less than the number of morphologically apoptotic cells, there were significant relations between both the severity of HI and delayed energy impairment measured by MRS, and the fraction of apoptotic cells estimated by ISEL ($P<0.025$). This is shown in Figure 5.

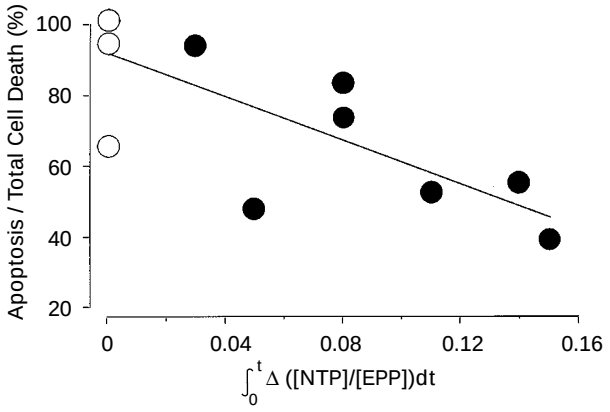

Figure 4 Relation between the proportion of total cell death that was apoptotic (apoptosis/total cell death) and the severity of hypoxia-ischaemia, as measured by the time integral of the fall in the ratio of nucleotide triphosphate: exchangeable phosphate pool ($_0\int^t\Delta$[NTP]/[EPP]dt). The least-square linear regression line is shown ($P<0.01$)

Discussion

This study showed linear relations between the severity of impaired cerebral energy metabolism both during and after HI, and the number of both apoptotic and necrotic cells in the cingulate gyrus. HI severe enough to reduce cerebral high energy phosphate concentrations to approximately zero was associated with the highest numbers of apoptotic cells. Very little necrosis was seen in controls or after mild HI, but approximately 50% of cells were necrotic after severe dephosphorylation. Apoptosis was more prominent in controls and after mild insults; the relative increase in controls is most likely due to the effects of prolonged periods of anaesthesia and ventilation while lying in the bore of the spectrometer, where perfect maintenance of physiological care is difficult and mild cerebral hypoxia-ischaemia is not unlikely.

Morphological analysis

Apoptosis and necrosis occur together in many brain regions following HI in the newborn piglet (Yue *et al*, 1996). The cingulate gyrus was selected for study because it forms a large proportion of the volume of interest within the volume of interest of the MR coil and thus contains the tissue from which the MR spectra are derived, but also because this region is susceptible to hypoxic-ischaemic injury (Yue *et al*, 1996).

Apoptosis and necrosis were distinguished by light microscopic analysis with H&E staining using standard morphological criteria. Electron microscopy confirmed apoptosis and necrosis at the sub-cellular level. Nuclear changes in apoptotic cells contrasted with those seen in necrosis. Cytoplasmic changes were less easy to interpret since the cytoplasm of healthy cells was comparatively electron dense, but characteristic cytoplasmic vacuoles without organelle degradation were observed in apoptotic

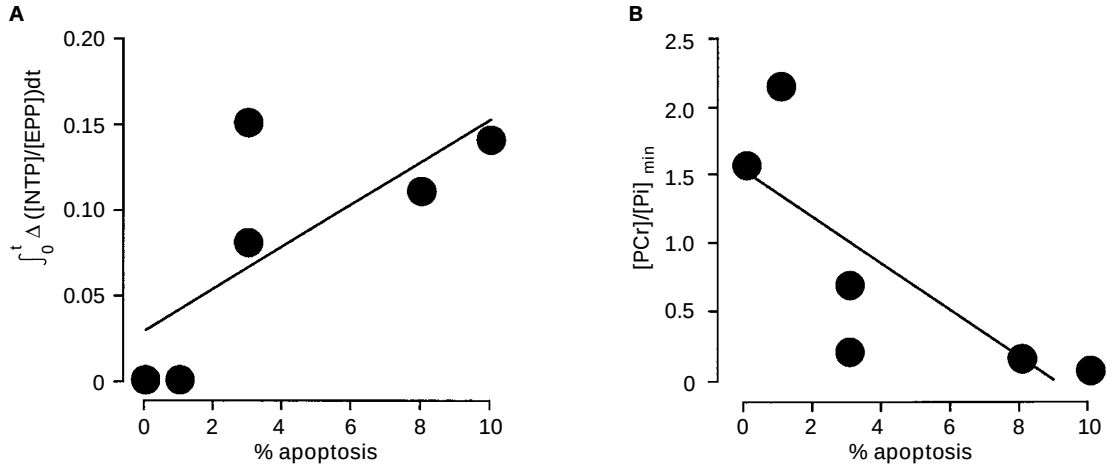

Figure 5 Relation between the proportion of cells stained positive by *in situ* end labelling of fragmented DNA and (**A**) the severity of hypoxia-ischaemia, as measured by the time integral of the fall in the ratio of nucleotide triphospate: exchangeable phosphate pool ($_0\int^t\Delta$[NTP]/[EPP]dt); (**B**) the decline in phosphocreatine: inorganic phosphate ([PCr]/[Pi]) during the delayed phase of injury

cells, while necrotic cells showed marked subcellular disintegration.

The present study did not type the dead cells, although some apoptotic cells could be provisionally characterised by simple morphology, and on this basis apoptosis appeared to occur in neurons, glia and endothelial cells. Further studies to characterise the susceptible cell lineages using immunocytochemical techniques are in progress.

In previous studies we have used *in situ* end-labelling (ISEL) of fragmented DNA to detect apoptotic cells. We demonstrated by this technique that pyknotic cells with reduced cytoplasm contained fragmented DNA, thus showing that the dense nuclear basophilia seen in these cells was due to apoptosis and was not artefactual. However, although a similar relation between ISEL-positive cells and impaired energy metabolism was found, the total numbers of cells detected by ISEL was less than using H&E and morphological criteria (Mehmet *et al*, 1994). Neither the single-strand or double-strand DNA polymerase method was able to detect all apoptotic cells without additional consideration of cell morphology. In particular, many karyorrhectic cells which were clearly apoptotic were not labelled, probably due to DNA degradation or packaging. A few necrotic cells were also labelled using this method. Other studies have found similar inconsistencies with end-labelling methods (Ravirajan *et al*, 1996). The results of the present study confirmed that ISEL detected fewer cells as apoptotic than morphological analysis, but also showed that there was a significant relation between the fraction of ISEL positive cells and the severity of cerebral injury measured by MRS.

Cerebral energy metabolism

The porcine model of hypoxic-ischaemic injury reproduced the metabolic derangements seen after human perinatal HI (Azzopardi *et al*, 1989; Martin *et al*, 1996; Hanrahan *et al*, 1996): reduced concentrations of high energy phosphates and increased Lac were observed during HI and again during a delayed phase of injury; pH_i fell during HI but not during delayed energy depletion (Lorek *et al*, 1994; Penrice *et al*, 1997). The metabolic consequences of HI were variable, providing a dynamic range of injury from moderate to very severe which was precisely quantitated by MRS. The decline in [PCr]/[Pi] seen in the more severely affected subjects was similar to that seen in infants who develop major neurodevelopmental impairment or die following birth asphyxia, confirming that HI was severe in these animals (Azzopardi *et al*, 1989).

Both [PCr]/[Pi] and [NTP]/[EEP] gave measures of the severity of impairment of oxidative phosphorylation. As the creatine kinase reaction preserves [NTP] at the expense of [PCr], [NTP]/[EPP] gave a more sensitive index of the severity of the acute insult because [PCr] fell to zero. Although use of [NTP]/[EPP] has a potential complexity in that a short severe insult could theoretically give a similar numerical value to less severe but prolonged dephosphoryation, the similarity of insult duration between subjects shows that this is not a confounding variable in this study. During delayed injury [NTP]/[EPP] was relatively preserved and thus [PCr]/[Pi] was the better index of impaired energy metabolism.

[Lac]/[Cr] increased during both phases of injury. The Cr peak includes both creatine and PCr and although the relative concentration of the components may change in a complimentary fashion following HI according to the creatine kinase reaction, total Cr should remain constant and is the best reference metabolite (Cady, 1994). The increase in [Lac]/[Cr] was thus due to an increase in Lac produced by glycolysis during ATP production. During HI this can be accounted for by deprivation of oxygen and was accompanied by intracellular acidosis. However in the secondary phase of injury high [Lac]/[Cr] together with normal or slightly alkaline pH_i is consistent with a relatively reduced intracellular redox state and a high $NADH/NAD^+$ ratio. Together with decreased [PCr]/[Pi] this demonstrates a significant impairment of mitochondrial function.

Relations between energy metabolism and the mode of cell death

Mitochondria play a complex role in the control of apoptosis. They participate directly in the apoptotic pathway as the site of action of CED-9/Bcl-2, CED-4 and CED-3/caspase activity and interaction (Chinnaiyan *et al*, 1997; Wu *et al*, 1997; Yang *et al*, 1997). Intracellular signals that induce mitochondrial membrane permeability transition may lead to release of cytochrome-c or apoptosis inducing factor which allows apoptosis to complete (Liu *et al*, 1996; Marchetti *et al*, 1996). High levels of Pi may promote membrane permeability transition (Kowaltowski *et al*, 1996).

However, mitochondrial ATP generation seems to be required for apoptosis to proceed (Wallen Ohman *et al*, 1993; Richter *et al*, 1996; Liu *et al*, 1996). Glutamate treatment of cerebellar granule neurons leading to persistent energy depletion causes rapid necrosis, but cells that recover mitochondrial function undergo apoptosis some hours later (Ankarcrona *et al*, 1995). These and other results obtained *in vitro* have suggested that a severe mitochondrial injury or ATP depletion in neural cells leads to necrosis, while a less intense stress induces apoptosis (Bonfoco *et al*, 1995).

Nevertheless, *in vivo* although necrosis became frequent after severe HI, the amount of apoptosis also increased and still accounted for approximately 50% of total cell death even after the most profound [NTP] depletion. This may be related to several factors. First, MRS data gave an integrated measure of energy metabolism, and did not detect heterogeneity in cell responses. Regional differences in physiological variables, such as: the matching of blood flow to energy requirements; the development of neurotransmitter systems and metabolic pathways; or cellular antioxidant capacity probably led to variability in the severity of injury within the brain. Our results are thus not incompatible with studies *in vitro*. Second, cell death sufficient to cause tissue destruction might impede substrate delivery to cells in the process of apoptosis, causing secondary necrotic death before the apoptotic programme could complete. The numbers of apoptotic cells observed may thus have represented a minimum number,

and the true number of cells triggered to undergo apoptosis might have been considerably higher. Third, HI triggers multiple complex mechanisms within intact tissue that may be difficult to replicate in cell culture. For example, extracellular glutamate concentrations increase not only during HI, but again during the delayed phase of injury, and the pathological effects may be different during these different periods of injury (Tan *et al*, 1996; Szatkowski and Attwell, 1994). Fourth, the loss of cells by necrosis might remove trophic support for other cells and precipitate them to apoptosis. For all these reasons it is not surprising that apoptosis and necrosis were frequently observed together.

These results show that apoptosis can be a quantitatively important consequence of severe as well as moderate HI in the developing brain. Since apoptosis is an active process that may be prevented by intervention before the commitment point, therapeutic intervention following perinatal HI might profitably be directed towards interrupting the apoptotic cascade.

Materials and Methods

Surgical preparation

Thirteen healthy term Large White piglets were studied on the first day of life. The experimental details for this model of transient global HI have been described elsewhere (Lorek *et al*, 1994). Briefly, after anaesthesia with midazolam, isoflurane and nitrous oxide a tracheostomy was formed amd mechanical ventilation established. Both common carotid arteries were isolated by remotely controlled vascular occluders (OC2A, In Vivo Metric, California, USA). Full circulatory and ventilatory support was provided for 48 h, with rectal temperature maintained between 38 and 39°C, which is normal for piglets. Eight animals were subjected to HI, and the remaining five were studied as sham-operated controls.

^{31}P and ^{1}H magnetic resonance spectroscopy

Animals were positioned within the 21 cm bore of a 7T Bruker Biospec (Bruker Medizintechnik, Karlsruhe, Germany) operating at 121.6 MHz for ^{31}P and 300.4 MHz for ^{1}H. Spectra were acquired continuously using a 25 mm-diameter double-tuneable surface coil centred on the intact scalp over the parietal lobes. Details of the MRS techniques used have been described in detail elsewhere (Lorek *et al*, 1994; Penrice *et al*, 1997).

Cerebral hypoxia-ischaemia

Once baseline measurements were completed cerebral HI was induced by occluding the carotid arteries and simultaneously reducing the FiO_2 to 12%. When [PCr]/[Pi] was either zero or very close to zero and [NTP]/[EPP] had fallen below 30% of baseline piglets were resuscitated by releasing the carotid occluders and providing an inspired oxygen concentration appropriate to normalise the arterial oxygen tension. The extent of acute cerebral energy depletion was quantified by the time integral of the decline in [NTP]/[EPP] during HI and in the first hour after resuscitation. Full intensive care and general anaesthesia were continued for a further 48 h from cerebral resuscitation, during which time interleaved ^{31}P and ^{1}H MRS observations were made repeatedly.

Harvesting and storage of tissue

At the end of the experiment animals were sacrificed by an overdose of anaesthetic and the carotid arteries cannulated immediately. Brains were perfused through these vessels with 100 ml phosphate buffered saline (PBS) followed by 100 ml 1% paraformaldehyde in PBS, surgically removed and fixed in 1% paraformaldehyde for 16 h at 4°C, then washed and transferred to a 15% (w/v) sucrose solution (in PBS) for storage at 4°C prior to mounting in paraffin blocks. In two animals tissue was taken from the cingulate prior to perfusion and placed in 2% gluteraldehyde (in PBS) for electron microscopic analysis.

Histological examination and cell counting

Coronal paraffin sections (5 μm) were cut and mounted on glass slides which had been coated with 2% 3-aminopropyltriethoxysilane (Sigma, Poole, Dorset, UK). Sections of the cerebral cortex containing the cingulate gyrus were dewaxed, rehydrated and stained by Cole's Haematoxylin and Eosin (H&E). The proportions of cells dying by apoptosis or necrosis were quantitated independently by an observer unaware of the experimental data. Counting was done usine a $\times 40$ objective and an eyepiece graticule with 100 grid squares (Olympus, Tokyo, Japan). Twenty fields were evaluated: ten to include the superficial cortex (layers II and III) and ten to include deeper layers (IV, V and VI) and a minimum of 1000 nuclei were counted. Apoptotic cells were identified using the following morphological criteria (Wyllie and Duvall, 1992): (1) intense, uniform nuclear basophilia; (2) chromatin condensation with nuclear shrinkage and pyknosis or (3) fragmentation of the nucleus into several rounded and uniformly densely basophilic masses (karyorrhexis). Necrotic cells were identified by the following morphological criteria: (1) intense cytoplasmic eosinophilia with; (2) reduced plasma and nuclear membrane integrity; or (3) dispersion of chromatin as a fine web into the cytoplasm, usually associated with increased cell volume. Cells showing irregular chromatin condensation at the nuclear periphery were excluded as indeterminate. The number of apoptotic or necrotic cells were expressed as the percentage of the total nuclei counted.

In situ end labelling (ISEL) was carried out essentially following the protocol of Ansari *et al* (1993) with the following modifications. Paraffin sections adjacent to HE stained sections were dewaxed, rehydrated and digested with 10 μg ml^{-1} proteinase K (Sigma, Poole, UK) at room temperature (RT) for 15 min. The end labelling mix (500 μl per section) contained 10 mM each of d-GTP, d-TTP and d-ATP and 4 mM biotin-14-dATP (Gibco BRL, Paisley, Scotland) in 50 mM Tris-HCl buffer (pH 7.5) supplemented with 5 mM $MgCl_2$, 10 mM 2-mercaptoethanol, 0.005% bovine serum albumin (fraction V, Sigma) and the Klenow fragment of DNA polymerase I (Pharmacia Biotech, Milton Keynes, UK) at 5 units/ml. Sections were incubated for 2 h at 37°C in humid chamber and the reaction was terminated by sequential washes in deionised water (three times) and 10 mM PBS (once). To block endogenous peroxidase, sections were immersed in 0.3% H_2O_2/PBS for 15 min at RT followed by four washes in PBS. Incorporated biotinylated nucleotides were detected with horseradish peroxidase (HRP) using a commercial kit (Vectastain, from Vector Laboratories, Peterborough, UK). Sections were then counterstained with Mayer's haematoxylin and mounted in DPX. For negative controls, Klenow Fragment of DNA polymerase I was omitted from the nucleotide mixture. For ISEL counts, apoptotic cells were defined as those with both the morphological characteristics described above and where the nucleus was HRP-positive.

Electron microscopy

Fresh tissue samples not exceeding 1 mm^3 in volume were fixed in 2% gluteraldehyde in PBS for 2 h at 4°C. After washing in PBS, tissues were osmicated and dehydrated in acidified DMP before routine embedding in Taab resin. One μm sections were cut and stained with toluidine blue for observation by light microscopy. Following selection of relevant blocks, ultra thin sections of approximately 100 nm were collected on nickel grids and stained with uranyl acetate and lead citrate for electron microscopic examination (Philips, CM-10, Eindhoven, Netherlands).

Statistical considerations

Data distributions were investigated for normality, and parametric or non-parametric tests used as appropriate. Differences between group means were tested by analysis of variance with Student-Newman-Keul's or Dunn's multiple comparison test. Relations between continuous variables was tested by linear regression analysis when appropriate. It was predicted *a priori* that there would be significant multicollinearity between MRS measures of energy metabolism which interrogated the same biological process. Consequently multivariate linear regression analysis was not performed, instead the informative univariate analyses are presented, and because of this significance testing was only regarded as significant if the value of p was less than 0.025.

Acknowledgements

Supported by the Wellcome Trust (Grant number 03891/Z/93), the Weston Foundation and the Medical Research Council.

References

Ankarcrona M, Dypbukt JM, Bonfoco E, Zhivotovsky B, Orrenius S, Lipton SA and Nicotera P (1995) Glutamate-induced neuronal death: a succession of necrosis or apoptosis depending on mitochondrial function. Neuron. 15: 961 – 973

Ansari B, Coates PJ, Greenstein BD and Hall PA (1993) In situ end-labelling detects DNA strand breaks in apoptosis and other physiological and pathological states. J. Pathol. 179: 1 – 8

Azzopardi D, Wyatt JS, Cady EB, Delpy DT, Baudin J, Stewart AL, Hope PL, Hamilton PA and Reynolds EO (1989) Prognosis of newborn infants with hypoxic-ischemic brain injury assessed by phosphorus magnetic resonance spectroscopy. Pediatr. Res. 25: 445 – 451

Beilharz E, Williams CE, Dragunow M, Sirimanne E and Gluckman PD (1995) Mechanisms of cell death following hypoxic-ischaemic injury in the immature rat: evidence of apoptosis during selective neuronal loss. Mol. Brain Res. 29: 1 – 14

Blumberg RM, Cady EB, Wigglesworth JS, McKenzie JE and Edwards AD (1996) Relation between delayed impairment of cerebral energy metabolism and infarction following transient focal hypoxia ischaemia in the developing brain. Exp. Brain Research 113: 130 – 137

Bonfoco E, Krainc D, Ankarcrona M, Nicotera P and Lipton SA (1995) Apoptosis and necrosis: two distinct events induced, respectively, by mild and intense insults with N-methyl-D-aspartate or nitric oxide/superoxide in cortical cell cultures. Proc Natl Acad Sci USA 92: 7162 – 7166

Cady E (1994) Metabolite concentrations and relaxation in perinatal cerebral hypoxic-ischaemic injury. Neurochem Res. 21: 1049 – 1058

Chariaut-Marlangue C, Margaill I, Plotkine M and Ben-Ari Y (1995) Early endonuclease activation following reversible focal ischemia in the rat brain. J. Cereb. Blood Flow Metab. 15: 385 – 388

Chinnaiyan AM, O'Rourke K, Lane BR and Dixit VM (1997) Interaction of CED-4 with CED-3 and CED-9: a molecular framework for cell death. Science 275: 1122 – 1126

Edwards AD, Yue X, Cox P,Hope PL, Azzopardi D, Squier MV and Mehmet H (1997) Apoptosis in the brains of infants suffering intrauterine cerebral injury. Pediatr. Res. 42:

Hanrahan D, Sargentoni J, Azzopardi D, Manji K, Cowan F, Rutherford MA, Cox IJ, Bell JD, Bryant D and Edwards AD (1996) Cerebral metabolism within 18 hours of birth asphyxia: a proton magnetic resonance spectroscopy study. Pediatr. Res. 39(4): 584 – 590

Kowaltowski AJ, Castilho RF and Vercesi AE (1996) Opening of the mitochondrial permeability transition pore by uncoupling or inorganic phosphate in the presence of Ca2+ is dependent on mitochondrial-generated reactive oxygen species. FEBS Lett. 378: 150 – 152

Li Y, Chopp M, Jiang N, Yao F and Zaloga C (1995) Temporal profile of in situ DNA fragmentation after transient middle cerebral artery occlusion in the rat. J. Cereb. Blood Flow Metab. 15: 389 – 397

Linnik MD, Zobrist RH and Hatfield MD (1993) Evidence supporting a role for programmed cell death in focal cerebral ischaemia in rats. Stroke 24: 2002 – 2008

Liu X, Kim CN, Yang J, Jemmerson R and Wang X (1996) Induction of apoptotic program in cell-free extracts: requirement for dATP and cytochrome c. Cell 86: 147 – 157

Lorek A, Takei Y, Cady EB, Wyatt JS, Penrice J, Edwards AD, Peebles DM, Wylezinska M, Owen-Rees H, Kirkbride V, Cooper C, Aldridge RF, Roth SC, Brown G, Delpy DT and Reynolds EOR (1994) Delayed ('secondary') cerebral energy failure following acute hypoxia-ischaemia in the newborn piglet: continuous 48-hour studies by 31P magnetic resonance spectroscopy. Pediatr. Res. 36: 699 – 706

MacManus JP, Buchan AM, Hill IE, Rasquinha I and Preston E (1993) Global ischaemia can cause DNA fragmentation indicative of apoptosis in rat brain. Neurosci Lett. 164: 89 – 92

Macmanus JP, Hill IE, Preston E, Rasquinha I, Walker T and Buchan AM (1995) Differences in DNA fragmentation following transient cerebral or decapitation ischemia in rats. J. Cereb. Blood Flow Metab. 15: 728 – 737

Marchetti P, Castedo M, Susin SA, Zamzami N, Hirsch T, Macho A, Haeffner A, Hirsch F, Geuskens M and Kroemer G (1996) Mitochondrial permeability transition is a central coordinating event of apoptosis. J. Exp. Med. 184: 1155 – 1160

Martin E, Buchli R, Ritter S, Schmid R, Largo RH, Boltshauser E, Fanconi S, Duc G and Rumpel H (1996) Diagnostic and prognostic value of cerebral 31P magnetic resonance spectroscopy in neonates with perinatal asphyxia. Pediatr. Res. 40: 749 – 758

Mehmet H, Yue X, Squier MV, Lorek A, Cady E, Penrice J, Sarraf C, Wylezinska M, Kirkbride V, Cooper C, Brown GC, Wyatt JS, Reynolds EOR and Edwards AD (1994) Increased apoptosis in the cingulate sulcus of newborn piglets following transient hypoxia-ischaemia is related to the degree of high energy phosphate depletion during the insult. Neurosci. Lett. 181: 121 – 125

Penrice J, Lorek A, Cady EB, Amess P, Wylezinska M, Cooper CE, D'Souza P, Brown GC, Kirkbride V, Edwards AD, Wyatt JS and Reynolds EOR (1997) Proton magnetic resonance spectroscopy of the brain during acute hypoxia-ischemia and delayed cerebral energy failure in the newborn piglet. Pediatr. Res. 41: 795 – 802

Petroff OA, Richard JW, Behar KL, Alger JR, den Hollander JA and Shulman RG (1985) Cerebral intracellular pH by 31P nuclear magnetic resonance spectroscopy. Neurology 35: 781 – 788

Ravirajan CT, Sarraf CE, Anilkumar TV, Golding MC, Alison MR and Isenberg DA (1996) An analysis of apoptosis in lymphoid organs and lupus disease in murine systemic lupus erythematosus (SLE). Clin. Exp. Immunol. 105: 306 – 312

Richter C, Schweizer M, Cossarizza A and Franceschi C (1996) Control of apoptosis by the cellular ATP levels. FEBS Lett. 378: 107 – 110

Roth SC, Edwards AD, Cady EB, Delpy DT, Wyatt JS, Azzopardi D, Baudin J, Townsend J, Stewart AL and Reynolds EOR (1992) Relation between cerebral oxidative metabolism following birth asphyxia and neurodevelopmental outcome and brain growth at one year. Dev. Med. Child Neurol. 34: 285 – 295

Szatkowski M and Attwell D (1994) Triggering and execution of neuronal death in brain ischaemia: two phases of glutamate release by different mechanisms. Trends Neurosci. 17: 359 – 365

Tan WK, Williams CE, During MJ, Mallard CE, Gunning MI, Gunn AJ and Gluckman PD (1996) Accumulation of cytotoxins during the development of seizures and edema after hypoxic-ischaemic injury in late gestation fetal sheep. Pediatr. Res. 39(5): 791 – 797

Vannucci RC, Yager JY and Vannucci SJ (1994) Cerebral glucose and energy utilization during the evolution of hypoxic-ischemic brain damage in the immature rat. J. Cereb. Blood Flow Metab. 14: 279 – 288

Wallen Ohman M, Lonnbro P, Schon A and Borrebaeck CA (1993) Antibody-induced apoptosis in a human leukemia cell line is energy dependent: thermochemical analysis of cellular metabolism. Cancer Lett. 75: 103 – 109

Wu D, Wallen D and Nunez G (1997) Interaction and regulation of subcellular localisation of CED-4 and CED-9. Science 275: 1126 – 1129

Wyllie AH and Duvall E (1992) Cell injury and death. In: McGee JO, Isacsson PG, Wright NA (eds) Oxford Textbook of Pathology. Oxford University Press, Oxford, pp 141 – 193

Yang J, Liu X, Bhalla K, Kim CN, Ibrado J, Cai J, Peng T, Jones DP and Wang X (1997) Prevention of apoptosis by Bcl-2: release of cytochrome c from mitochondria blocked. Science 275: 1129 – 1132

Yue X, Mehmet H, Penrice J, Cooper C, Cady E, Wyatt JS, Reynolds EOR, Edwards AD and Squier MV (1996) Apoptosis and necrosis in the newborn piglet brain following transient cerebral hypoxia-ischaemia. Neuropathol. Appl. Neurobiol. 22: 482 – 503